International Research Journal of Multidisciplinary Scope (IRJMS), 2025; 6(3):1014-1029 IRJMS

Original Article | ISSN (O): 2582-631X DOI: 10.47857/irjms.2025.v06i03.04551

Multifaceted Characterization of Diglycine Picrate (DGP) Single Crystals: Exploring Growth, Mechanical, Optical, Thermal, Electrical, and Laser Damage Threshold Properties for Advanced Nonlinear Optical Applications

R Suganthi*, K Balasubramanian

Department of Physics, M.D.T. Hindu College (Affiliated to Manonmaniam Sundaranar University, Abishekapatti – 627012, Tirunelveli), Pettai, Tirunelveli -10, Tamil Nadu, India. *Corresponding Author's Email: jerusharma2014@gmail.com

Abstract

A pure Diglycine picrate (DGP) single crystal was successfully grown using the slow evaporation solution technique from a 2:1 molar mixture of glycine and picric acid dissolved in distilled water. The crystal growth process yielded high-quality crystals suitable for detailed analysis. Single-crystal X-ray diffraction (XRD) was employed to determine the crystal structure and unit cell parameters, confirming the monoclinic system. Powder XRD analysis further verified the phase purity and crystallinity of the grown crystal. FTIR spectroscopy was utilized to identify the functional groups and confirm molecular interactions within the crystal lattice. Mechanical stability was assessed using Vickers microhardness testing, revealing adequate hardness suitable for device applications. Optical properties, including transmission and absorption behavior, were studied through UV–visible–near-infrared spectroscopy, demonstrating excellent transparency with a sharp cut-off wavelength. Thermal stability and decomposition temperature were analyzed using thermogravimetric and differential thermal analysis (TG/DTA), indicating stability up to 240 °C. Dielectric measurements showed frequency-dependent variations in dielectric constant and loss, reflecting low dielectric loss at higher frequencies. The laser damage threshold (LDT) was evaluated using a Nd:YAG laser at 1064 nm, demonstrating the crystal's robustness under high-intensity irradiation. Third-order nonlinear optical susceptibility was investigated via the Z-scan technique, highlighting the DGP crystal's promising nonlinear optical properties. These comprehensive studies establish the potential of DGP crystals for advanced nonlinear optical device applications.

Keywords: FTIR, LDT, TG-DTA, UV, XRD, Z-Scan Analysis.

Introduction

Organic nonlinear materials have proven to be sustainable materials with a valuable and numerous range of applications in semiconductors, superconductors, and nonlinear optical devices. Currently, organic NLO crystals are employed in more advanced technical applications compared to inorganic crystals, because organic nonlinear optical crystals can exhibit advantageous chemical, mechanical, optical, and electrical properties that are much needed for diverse applications. Good organic NLO crystals are used for optoelectronic devices. Nonlinear optical (NLO) materials play a crucial role in modern photonic and optoelectronic technologies due to their ability to interact with intense light fields and generate new frequencies (1). These materials have become indispensable in applications such as laser frequency conversion, telecommunications, optical switching, and signal processing. Organic NLO crystals are especially promising for third-order nonlinear optical processes, such as third harmonic generation (THG), due to their large polarizabilities and delocalized π-electron systems. The continued demand for novel, efficient, and sustainable NLO materials has led researchers to explore simple organic molecules that can be functionalized to exhibit enhanced nonlinear responses. Glycine, the most basic stable amino acid, possesses a solitary hydrogen atom as its side group. The basic organic component of glycine can react with acids, inorganic-organic salts, and other compounds to produce suitable NLO materials. Picric acid is a pale yellow-coloured and odourless crystal that is soluble in distilled water, organic solvents, and chloroform. Picric acid has active π and ionic inter-

(Received 19th March 2025; Accepted 09th July 2025; Published 27th July 2025)

actions; it interacts with organic and amino acids to make useful NLO picrates (2, 3). The mixture of glycine and picric acid produces a good NLO material with third harmonic generation capability. Numerous studies have focused on amino acid-based NLO materials, with glycine being one of the most commonly explored due to its zwitterionic nature and strong hydrogen bonding ability. Compounds such as diglycine nitrate and triglycine sulfate have been extensively studied for their NLO activity and dielectric properties. However, these crystals often suffer from limitations such as low thermal stability, limited optical transparency, and poor mechanical hardness, which restrict their applicability in high-power laser systems and integrated photonic devices. Previous research has demonstrated that the combination of picric acid with amino acids can lead to the formation of stable NLO materials with desirable optical and thermal characteristics. However, systematic studies comparing these materials are still limited, particularly those that assess third-order NLO behavior using modern characterization techniques.

Despite the promising properties of amino acid–based and picrate–based NLO materials, there is still a lack of comprehensive studies that investigate their structural, thermal, mechanical, optical, and third-order nonlinear properties in a single framework. Most earlier works have focused on isolated properties or limited characterization, which makes it difficult to assess the true potential of these materials for integrated applications. Furthermore, the synergistic effects of combining glycine with picric acid to form diglycine picrate (DGP) remain underexplored, especially in terms of Z-scan studies for third-order NLO coefficients, dielectric behavior, and laser damage threshold analysis.

This study aims to develop a novel third-order nonlinear optical (NLO) material—diglycine picrate (DGP)—with enhanced third harmonic generation capabilities. High-quality single crystals of DGP are grown using the slow evaporation method and subjected to comprehensive characterization. Structural properties are determined using single-crystal and powder X-ray diffraction (XRD), while molecular vibrations are analyzed via Fourier-transform infrared (FTIR) spectroscopy. Optical transparency and band gap are assessed through UV–Vis–NIR spectroscopy, and mechanical strength is evaluated using microhardness testing. Thermal stability is examined using thermogravimetric and differential thermal analysis (TG/DTA). Dielectric properties are studied across various frequencies, and third-order NLO behavior is evaluated through laser damage threshold (LDT) testing and Z-scan analysis.

Novelty and Contribution of the Present Work

Compared to other glycine-based NLO crystals, such as diglycine nitrate and triglycine sulfate, DGP demonstrates superior thermal stability and enhanced third-order nonlinear optical response. This is attributed to the strong electron-withdrawing nitro group present in the picric acid moiety, which improves charge transfer efficiency. Furthermore, DGP exhibits broader UV transparency than glycine sodium nitrate, increasing its potential for photonic and optoelectronic applications (4, 5). The excellent NLO material diglycine picrate features a monoclinic crystal structure. This study introduces diglycine picrate (DGP) as a novel organic NLO crystal that offers significant improvements over previously reported glycine-based compounds. The novelty of this work lies in its holistic approach: DGP is not only synthesized and structurally analyzed, but also subjected to a suite of advanced characterizations that collectively demonstrate its suitability for high-performance NLO applications. The Z-scan analysis in particular provides rare insights into its third-order NLO behavior, filling a crucial gap in the literature**.** As a result, DGP positions itself as a strong candidate for future applications in nonlinear photonics, laser modulation, and optical signal processing.

Methodology

Synthesis

The synthesis of a Diglycine picrate single crystal began with the addition of picric acid and glycine in a 2:1 molar ratio. To achieve a uniform solution, glycine and picric acid were blended with distilled water and vigorously mixed with a magnetic stirrer device for eight hours. Continuous stirring was maintained throughout the process to obtain pure Diglycine picrate salt. After that, the mixture was allowed to evaporate freely at normal temperature. Fourteen days

later, the clear DGP crystal was extracted tilizing the slow evaporation solution method.

Crystal Growth

The synthesis of DGP crystal involved combining glycine with picric acid in a 2:1 molar ratio. Both components were accurately measured and dissolved individually in distilled water using separate beakers. After complete dilution, the solutions were gently mixed together for proper reaction and stirred at ambient temperature for eight hours using magnetic stirrer. The resulting blended solution exhibited a yellow colour, indicating the onset of the reaction. Following this, the formulated solution was set aside to vaporize freely at ambient temperature. Through this process, a light-yellow crystalline salt of the DGP single crystal was formed as a result of the appropriate chemical reaction. The well-grown DGP single crystals attained dimensions of 10 x9 x5 mm^3 and were harvested after 14 days. Figure 1 illustrates the appearance of the DGP crystal.

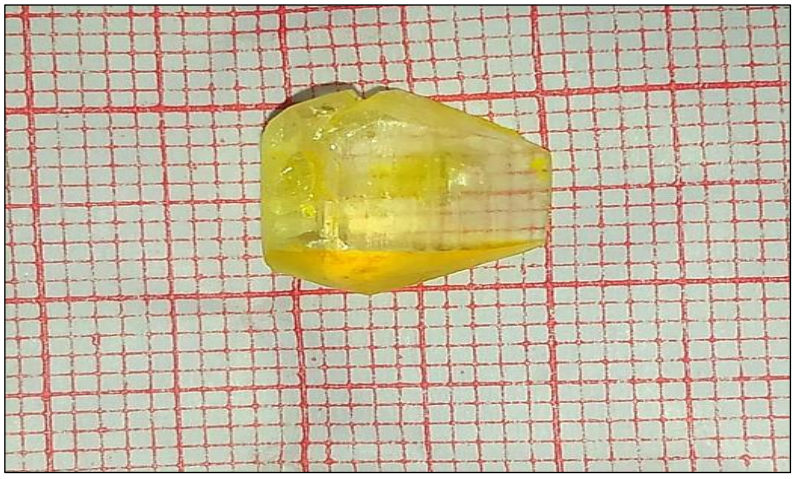

Figure 1: Picture of DGP

Table1: SC-XRD Results for DGP Crystal

Crystal	Lattice dimensions	Volume (Å)^3	Z
Diglycine Picrate (DGP) single crystal	a=15.142Å b=6.654 Å c=15.367 Å α=90^0; β=93^0 γ=90^0	1541.47	2

Results and Discussion

XRD Investigation

XRD is an essential approach for elucidating the structure of crystalline substances, as it enables the determination of the arrangement of individual atoms within a single crystal and provides information about lattice parameters (6). The DGP crystal undergoes single crystal - XRD investigation to ascertain the unit cell dimensions. The crystalline structure of DGP is classified under the centrosymmetric space group P21/c. Utilizing SC-XRD data, the monoclinic system was identified, revealing the reported cell dimensions: a=15.142(1) Å, b=6.654(2) Å, c=14.367(2) Å, with a unit cell volume of 1541.47 Å^3. Detailed SC- XRD data for the DGP single crystals are listed in Table 1.

Powder XRD Evaluation

PXRD investigation is employed to examine the diffraction pattern of crystalline materials. In this method, the crystallized substance is finely powdered and subjected to PXRD investigation. The crystalline integrity of the DGP crystal is verified by the presence of high-intensity peaks in its powder XRD spectrum. By scrutinizing the reflections at various angles depicted in the graph, it is noted that a particularly intense peak occurs at an angle of 29.724^0. These significant diffraction peaks at specific 2θ values signify the superior crystalline quality exhibited by the DGP single

crystal. The PXRD data for DGP is detailed in Table 2, while Figure 2 displays the (hkl) indexing spectra of the DGP single crystal. Table 3 presents the reflection peaks, their relative intensities, and corresponding 2θ values in the powder XRD pattern.

Table 2: PXRD Results of DGP Single Crystal

Pos.[◦2Th.]	Height[cts]	FWHM[◦2Th.]	d-Spacing[Å]	Rel.int.[%]
14.693	4665.23	0.063	6.02394	16.3
18.852	1052.29	0.131	4.70341	3.7
20.040	1122.23	0.107	4.42714	3.9
23.783	2770.94	0.116	3.73822	9.7
25.268	213.932	0.113	3.52176	0.7
28.239	513.998	0.148	3.15768	1.8
29.071	1430.98	0.110	3.60920	5.0
29.724	28568.7	0.060	3.00319	100
35.368	1075.27	0.130	2.53581	3.8
45.409	88.0014	0.055	1.99573	0.3
61.925	442.538	0.062	1.49726	1.5

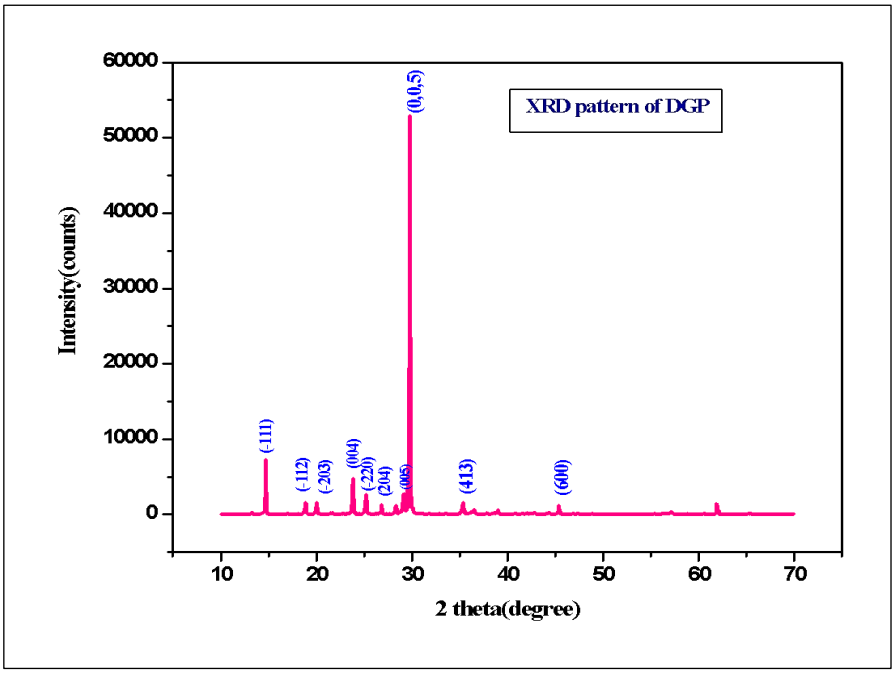

Figure 2: (hkl) Indexing Spectra of DGP

Table 3: PXRD Peaks for DGP

Peak No.	2theta(degrees)	Relative Intensity (%)	(hkl)
1.	14.693	16.3	-111
2.	18.852	3.7	-112
3.	20.040	3.9	-203
4.	23.783	9.7	004
5.	25.268	0.7	-220
6.	28.239	1.8	204
7.	29.724	100	005
8.	35.368	3.8	413
9.	45.409	0.3	600

FTIR Characterization

FTIR analysis is a good analysing tool for identifying molecules. The amount of infrared radiation absorbed by a sample which can be measured by FTIR analysis. The absorption bands corresponding to the vibrational modes of the DGP crystal can be identified through FTIR spectroscopy (7). The resulting spectrum can be employed for the identification of the functional moieties that are present in the molecule. Using the KBr pellet technique, the FTIR spectrum was obtained for the samples within the 500–4000 cm^{-1}range. Figure 3 depicts the DGP crystal's FTIR spectrum. The vibrational modes are listed in Table 4 align with the absorption bands in the spectrum of DGP. The following assignments pertain to various compound classes based on their wave numbers (cm^{-1}) and functional group modes. An O-H stretching vibration is detected at 3152.25 cm^{-1}, characteristic of alcohols. Aldehydes exhibit a C-H stretching mode at 2822.89 cm^{-1}, while carboxylic acids show an O-H stretching at 2605.42 cm^{-1}. The N=C stretching mode for isothiocyanates appears at 2098.21 cm^{-1}. Amine compounds display N-H bending at 1580.55 cm^{-1}, and nitro compounds feature N-O stretching at 1500.96 cm^{-1}. Alkanes are identified by C-H bending at 1442.86 cm^{-1}, whereas sulfoxides show S=O stretching at both 1407.11 cm^{-1} and 1031.84 cm^{-1}. Phenols are marked by O-H bending at 1329.71 cm^{-1}. Additionally, alkenes are characterized by C=C bending at 890.39 cm^{-1} and 694.56 cm^{-1}.

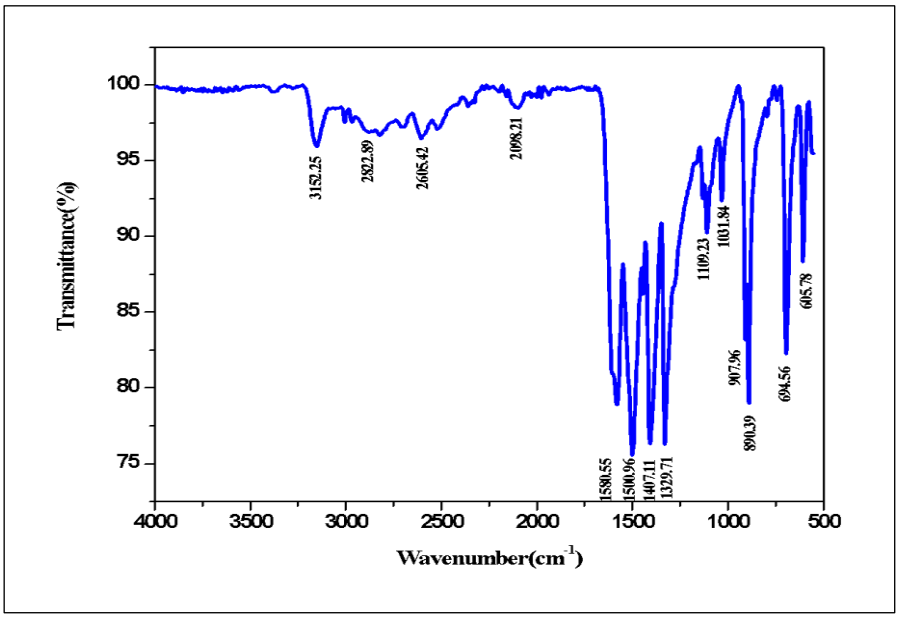

Figure 3: FTIR Curve of DGP

Table 4: Assigned Modes for DGP Wave Numbers

Wave Number (Cm^{-1})	Assignment Modes	Compound Class
3152.25	O-H stretching	Alcohol
2822.89	C-H stretching	Aldehyde
2605.42	O-H stretching	Carboxylic acid
2098.21	N=C=stretching	Isothiocyanate
1580.55	N-H bending	Amine
1500.96	N-O stretching	Nitro compound
1442.86	C-H bending	Alkane
1407.11	S=O stretching	Sulfoxide
1329.71	O-H bending	Phenol
1109.23	C-O stretching	Secondary alcohol
1031.84	S=O stretching	Sulfoxide
890.39	C=C bending	Alkene
694.56	C=C bending	Alkene

Hardness Analysis

Microhardness analysis is utilized to assess the surface hardness characteristics of materials at the microscopic level, a crucial consideration in device manufacturing due to its impact on mechanical properties (8). Transparent DGP single crystal samples, possessing flat and smooth surfaces, are employed for microhardness testing using Vicker microhardness with a diamond tip. Indentations are applied at different loads spanning from 25 grams to 100 grams. The Vicker hardness number for the developed DGP single crystal is computed employing the formula,

$$H_v = 1.8544\ P/d^2\ kg/mm^2 \ldots\ldots\ldots\ldots [1]$$

here 'P' denotes the applied load in kilograms and 'd' refers to the diagonal length in millimeters (9). A logarithmic plot of the applied load (log P) and diagonal length (log d) is depicted in Figure 4. The resulting DGP single crystal is categorized as hard, as evidenced by the calculated value of n (B=0.25943) derived from the graph. Figure 5 demonstrates the relation of hardness number to applied load, showing a linear increase in H_v from 25g to 50g, followed by a steady rise beyond 50g. Similarly, Figure 6 shows a plot between stiffness coefficient (C_{11}) and load, indicating a linear increase in hardness value with load from 25g to 100g. Figure 7 exhibits the relation between yield strength and load, revealing an increase in hardness value with increasing load after surpassing 50g, indicating a notable indentation size influence on the hardness of the DGP single crystal. Overall, these observations confirm that the DGP single crystal exhibits significant hardness, with increasing hardness and stiffness at higher loads. Such mechanical robustness is highly desirable for device fabrication, ensuring that the material can withstand physical processes such as cutting, polishing, and mounting without damage. This makes the DGP crystal not only mechanically stable but also highly suitable for integration into optoelectronic and nonlinear optical systems, where durability and precise handling are critical for long-term performance and reliability.

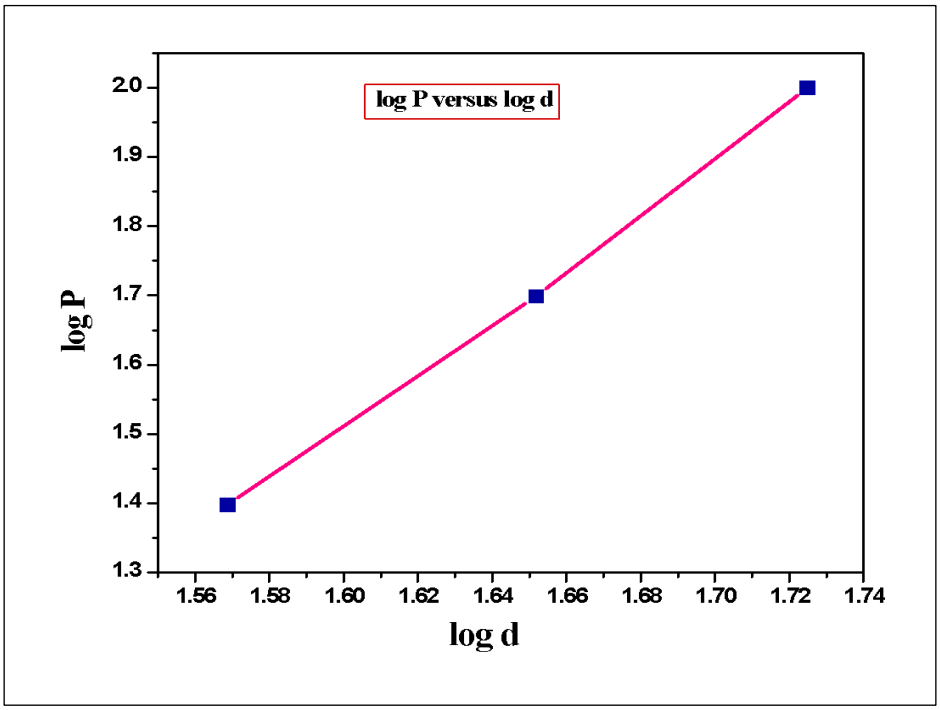

Figure 4: log P Versus log d

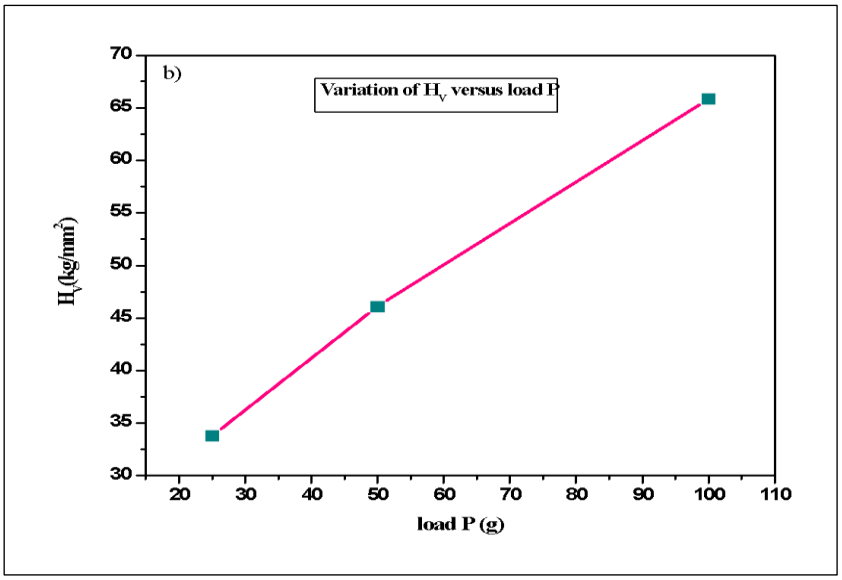

Figure 5: H_v Versus load P

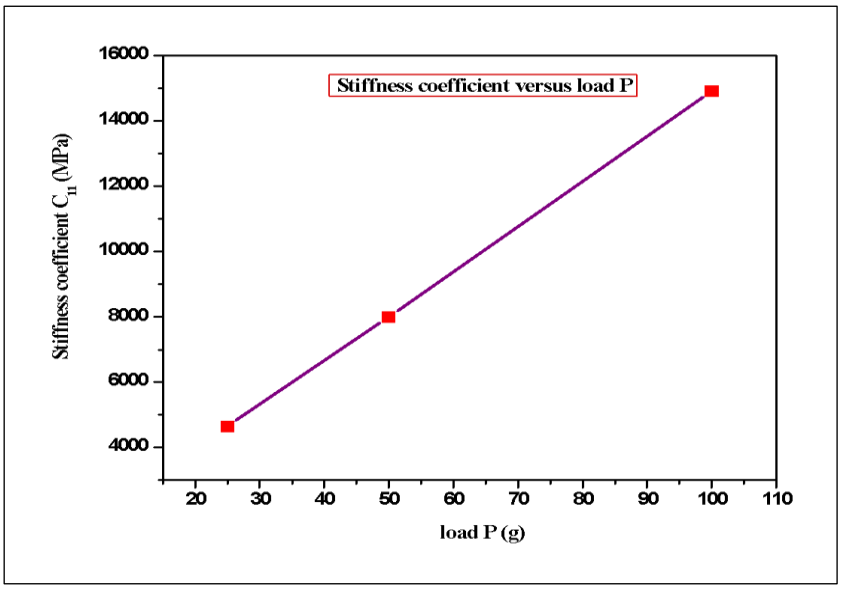

Figure 6: Stiffness Coefficient Versus load P

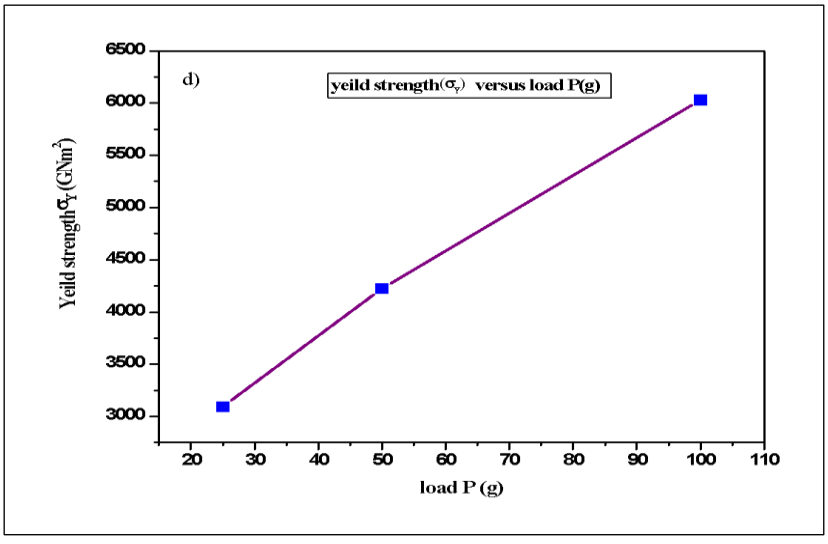

Figure 7: Yield Strength Versus load P

UV Analysis

UV-Vis spectroscopy relies upon the phenomenon where chemical compounds absorb UV or visible light, resulting in distinct spectra. UV spectroscopy is a subset of absorption spectroscopy that involves the absorption of ultraviolet light ranging from 200 to 400 nm by the molecule, resulting in the excitation of electrons from their basal state to elevated energy levels (10, 11). The transmittance of the DGP crystal was measured with an optical UV-visible-NIR spectrometer. Figure 8 shows the precise measurement of the optical band gap of DGP is 6 eV which can be found by means of extrapolation from linear section of the graph. The DGP crystal has broad transparency range between 400-1100nm in transmission spectra as shown in Figure 9. The observed transmission is nearly 98% in higher wavelength range. This represents the most valued attribute of the crystals for NLO applications. The increased depth which is favourable for more non-linear effect that observed in this DGP single crystal.

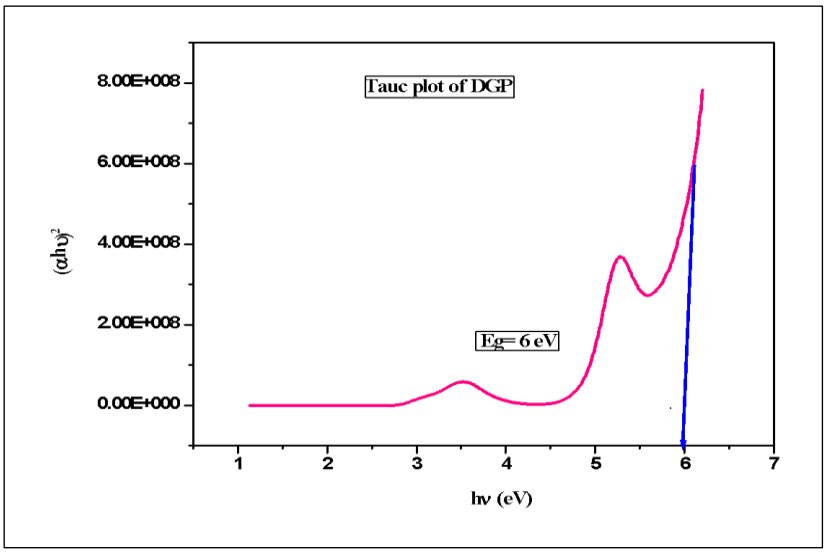

Figure 8: Tauc Plot of DGP

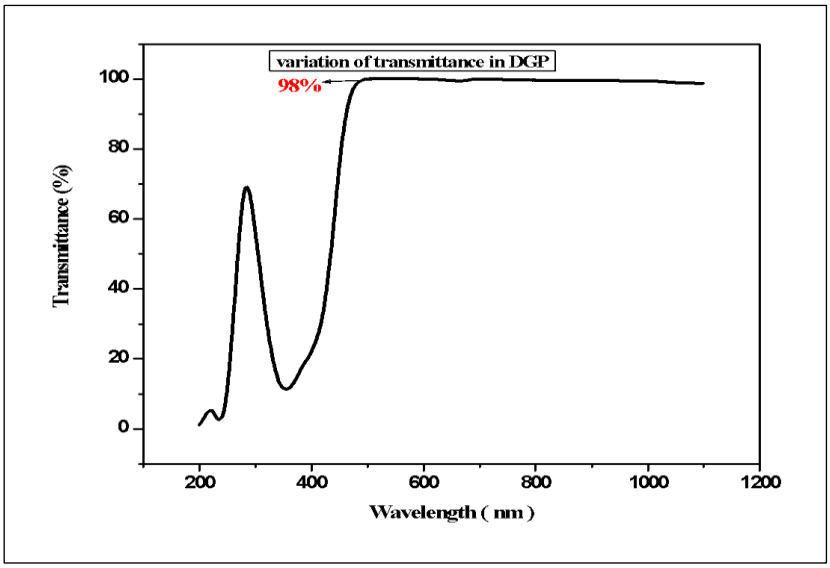

Figure 9: Transmittance Graph of DGP

Figure 10 shows the absorption of the DGP crystal, the UV cut-off wavelengths were detected at 235 nm and 350 nm, and it is because of the π-π* and n-π* transitions occurring in the DGP crystal. The variation of the extinction coefficient of DGP single crystal with wavelength is shown in Figure 11. The extinction coefficient is intricately connected to the absorption coefficient of the DGP single crystal. The minimum value of extinction coefficient occurs at a wavelength of 230nm, which corresponds to the

visible region (12). Hence the absorption of radiation in DGP single crystal will also be minimum in the visible spectrum. Figure 12 demonstrates that the enhancement of optical conductivity with incoming photon energy reflects a robust optical behavior of the DGP single crystal. The elevated value of optical conductivity (10^{9}-10^{12}) reveals an excellent photo response of the DGP single crystal. Figure 13 highlights the correlation between refractive index and wavelength. The lower value of refractive index is measured in the visible range as 0.2 for DGP single crystal. When wavelength rises, the refractive index decreases. The greater band gap, better transmission throughout the region and lower refractive index makes the DGP single crystal is a suitable tool for powerful optoelectronic applications.

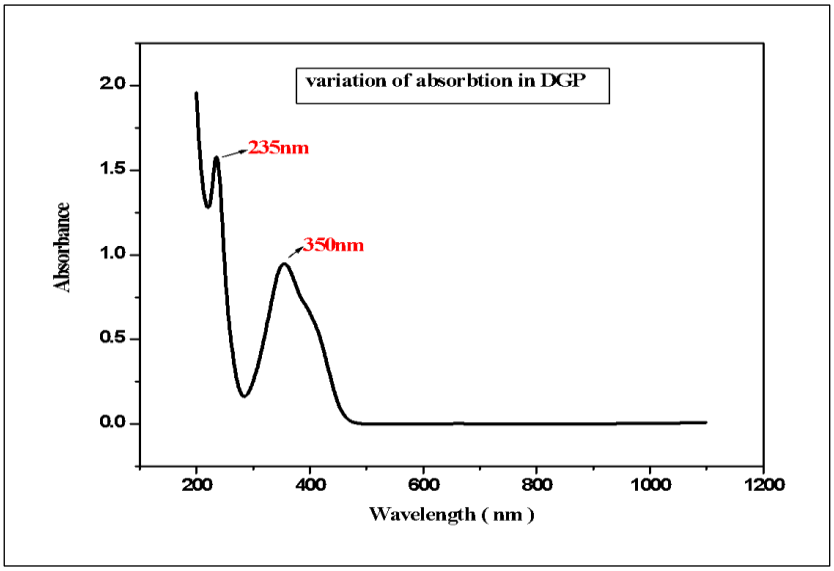

Figure 10: Absorption Spectrum of DGP

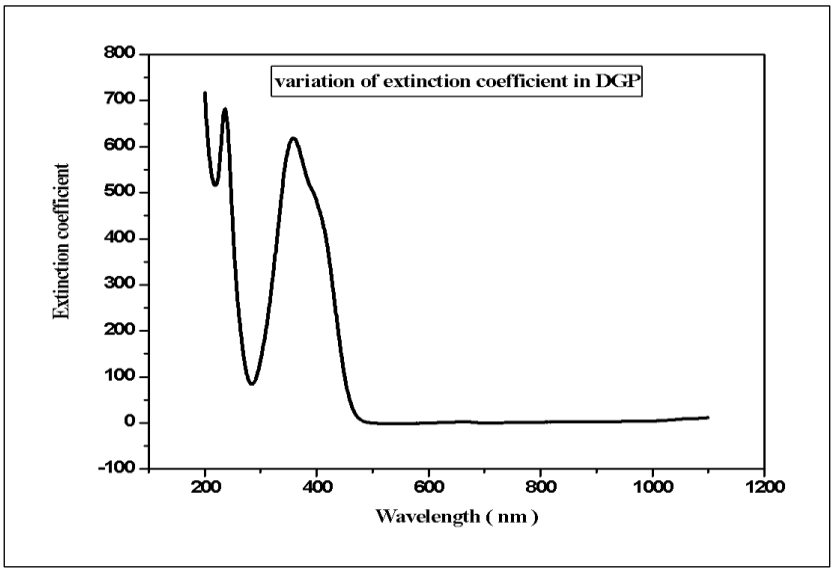

Figure 11: Extinction Coefficient of DGP

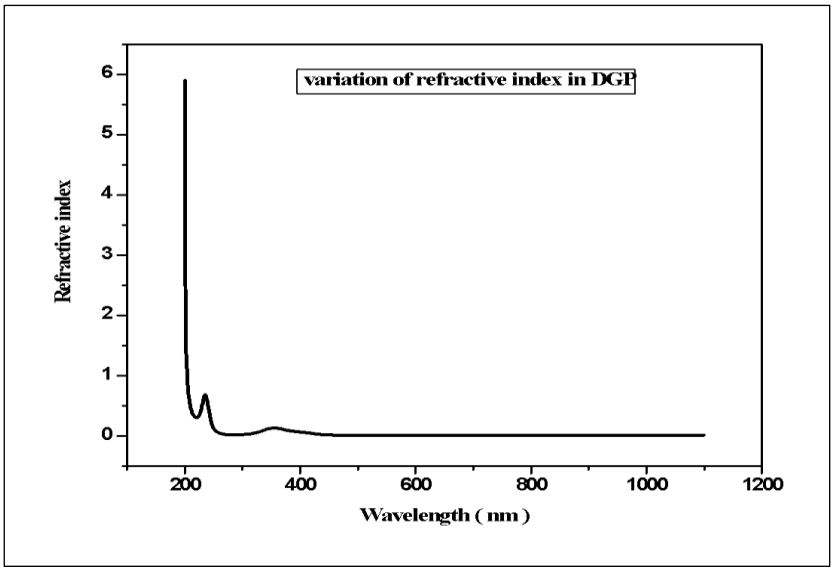

Figure 12: Optical Conductivity of DGP

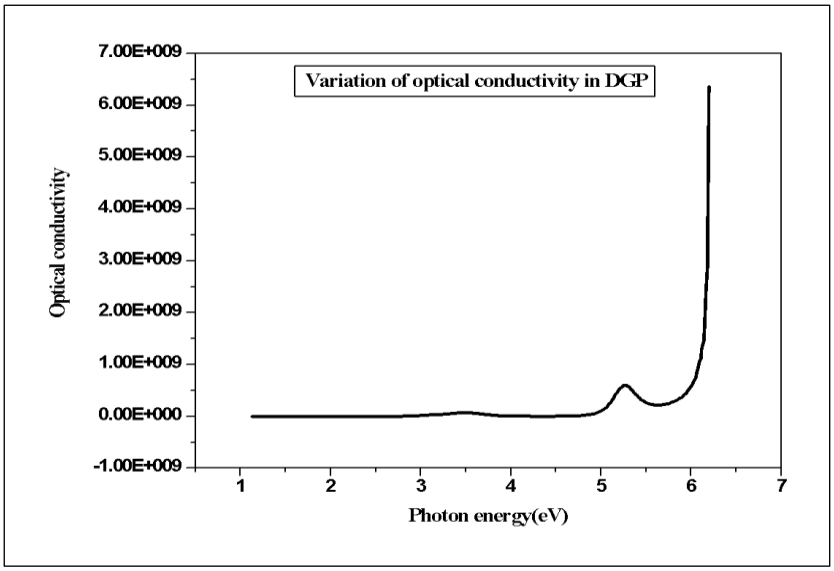

Figure 13: Refractive Index of DGP

Thermogravimetric Analysis

Thermo Differential Thermal Analysis-TG/DTA is a sophisticated thermal analysis technique adept at comprehensively evaluating diverse thermal properties of a crystal within a solitary experiment. The thermo-gravimetry component precisely measures the temperature at which decomposition, oxidation, or reduction occurs while concurrently monitoring weight variations caused by oxidation, decomposition, and associated physical and chemical changes leading to weight gain or loss. Meanwhile, the DTA component detects whether decomposition processes are endothermic or exothermic. Additionally, it records temperatures corresponding to phase transitions such as melting, crystallization, and glass transitions occur without any mass loss (13).TG/DTA studies were performed with a temperature range of 100°C to 800°C in a nitrogen environment, using a heating pace of 20°C per minute. The TG and DTA thermal behavior of the DGP single crystal is shown in Figure 14. The TG curve demonstrated that the DGP single crystal maintained thermal stability up to 250°C, with complete decomposition occurring at 280°C. This decomposition behavior is attributed to the breaking of hydrogen bonds and ionic interactions between diglycine and picrate ions. At elevated temperatures, thermal energy leads to fragmentation of the nitro-substituted aromatic ring in the picrate and degradation of the peptide backbone in diglycine, resulting in loss of

structural integrity. The DTA curve indicated a melting point at 275°C, followed by an endothermic transition (14). The pronounced endothermic peak in the DTA curve at 275°C confirms the high crystalline structure and integrity of the DGP crystal, as indicated by the distinctness of the peak.

Dielectric Testing

The dielectric features of a sample are influenced by the potential barrier present at its grain boundaries, which in turn diminishes space charge polarization. Consequently, at higher frequencies, there is a tendency for the dielectric constant to decrease, particularly at boundaries where accumulated charge is typically found (15). Figure 15 provides a visual representation of how the dielectric constant changes with frequency. The graph illustrates that the dielectric constant is greater at reduced frequencies but subsequently diminishes as the frequency rises.The observed lower dielectric permittivity at higher frequencies of the DGP crystal suggests a favorable conducting nature, indicating its potential for high optical quality in nonlinear optical (NLO) applications.

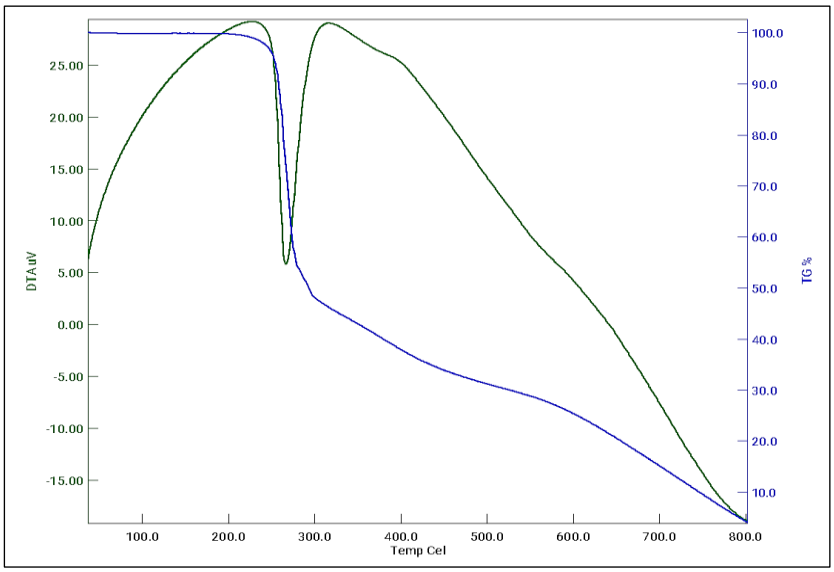

Figure 14: TG/DTA Spectrum for DGP

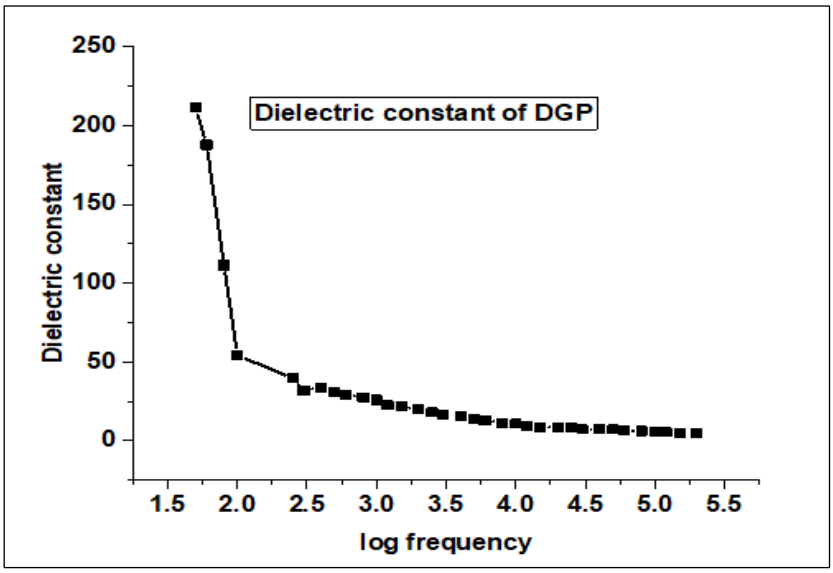

Figure 15: Variation of Dielectric Constant in DGP

Dielectric Loss

The evolved heat due to alternating the deposition of positive and negative charges in respective electrodes in capacitors has overcome through dielectric loss and it is measured as tangent angle (tanδ). Hence localized polarization causes the

lagging in Polarization. Therefore lagging in following the polarizing field is a measure of dielectric loss (16). Signal attenuation depends upon dielectric constant and dielectric loss by understanding the relation,

$$\text{Signal Attenuation} = 2.3 * f * \tan(\delta) * \sqrt{\varepsilon r} \quad \ldots\ldots\ldots\ldots\ldots [2]$$

Here 'f' signifies the frequency and 'εr' denotes the dielectric constant. Based on this relationship, it can be inferred that the DGP crystal demonstrates low dielectric loss at increased frequencies, indicating its potential adaptability for nonlinear optical (NLO) applications. Figure 16 shows the variation of dielectric loss with log f.

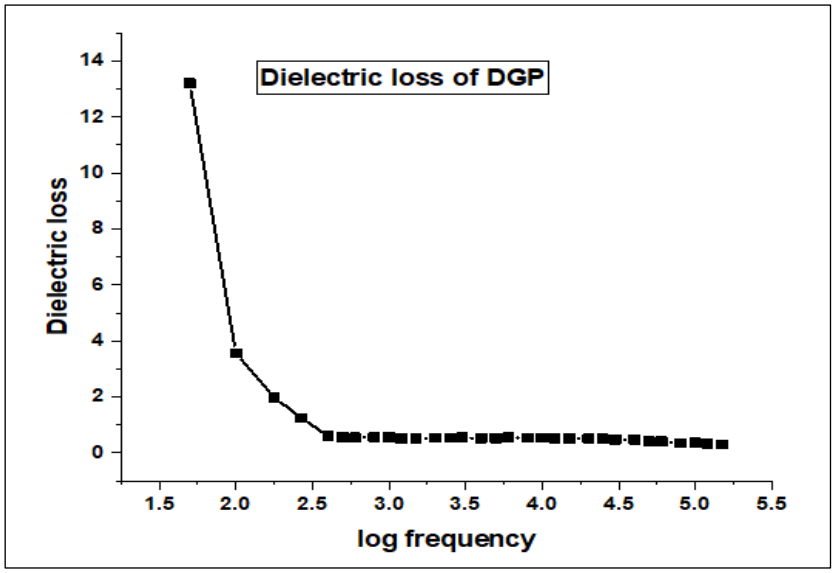

Figure 16: Variation of Dielectric Loss in DGP

Photoconductivity Evaluation

Photoconductivity in organic crystals is crucial for electronic and optoelectronic devices. These crystals, made of conjugated organic molecules, increase conductivity when exposed to light. Light absorption creates excitons, which can separate into free charge carriers under an electric field. Factors like molecular arrangement, crystal structure, and purity affect photoconductivity efficiency, impacting devices like solar cells and photodetectors (17). The photoconductivity of the pure DGP crystal was investigated at ambient temperature. Dark current (I_d) measurements were recorded incrementally from 0 to 50 V (DC) in the absence of illumination, while photocurrent (I_p) was measured under exposure to a 50 W halogen lamp. Figure 17 illustrates the variation of I_p and I_d with applied voltage. The DGP crystal exhibits positive photoconductivity, as evidenced by I_p exceeding I_d, which is likely due to the generation of mobile charge carriers through photon absorption. The photosensitivity of the DGP crystal was evaluated using a specific equation,

$$\text{Photosensitivity} = \frac{I_p - I_d}{I_d} \quad \ldots\ldots\ldots\ldots\ldots [3]$$

At 50 V, the DGP crystal showed a photosensitivity of 0.74, enhancing its conductivity under light by generating charge carriers efficiently. This property is key for technologies like organic solar cells and photodetectors. The crystal's tunable structure and high crystallinity improve its performance in optoelectronic applications.

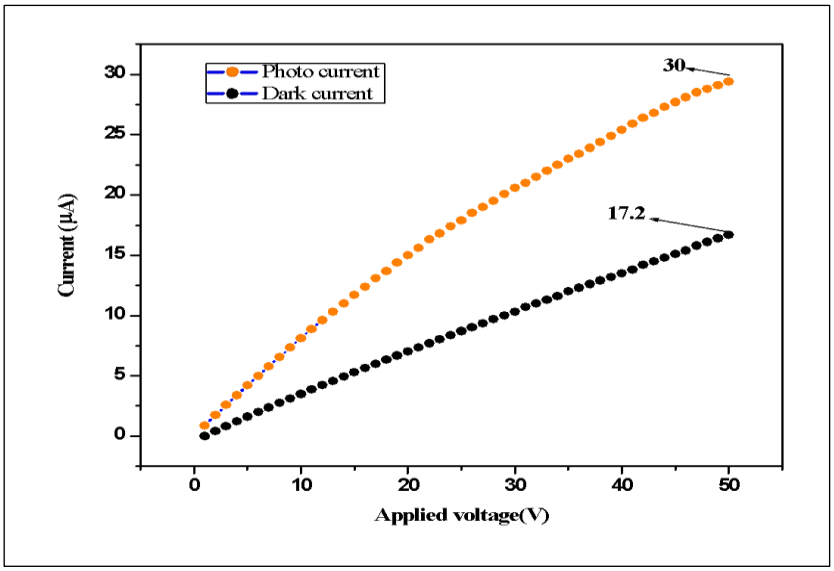

Figure 17: Photoconductivity of DGP Crystal

Laser Damaged Threshold Studies

The laser damage threshold (LDT) is the limit at which material will be damaged by giving the laser energy to the material in the form of intensity and wavelength of radiation.LDT values are essential for transmissive optical elements which can be used for applications where a laser-induced modification is required (18). In the case of DGP crystal, LDT investigation was conducted through a Q-switched high-energy Nd-YAG laser at 1064 nanometers from the Quanta Ray type. The laser radiation, with a pulse width of 6nanoseconds and wavelength of 1064 nanometers, impacted the sample at a frequency of 10 Hertz. The incident laser light had a focal length of 10 centimeters. The pulse energy of the incoming laser beam was quantified employing a power meter. Subsequently, the energy density was computed utilizing the equation (19),

$$\text{Power density, } P_d = E/\tau\pi r^{2.} \quad \ldots\ldots\ldots\ldots\ldots [4]$$

Here 'E' reflects the input energy density in millijoules, 'τ' denotes the pulse width in nanoseconds, and 'r' signifies the spot's radius in millimeters. The DGP crystal exhibits a remarkably elevated laser damage threshold of 3.36 GW/cm^2, surpassing that of KDP (0.20 GW/cm^2) and Urea (1.50 GW/cm^2) (20). Consequently, the DGP crystal shows a remarkable tolerance to optical damage. With its elevated LDT value, this single crystal can be fashioned for utilization in high-power laser devices (21). A comparison of the LDT of DGP with reported NLO crystals is shown in Table 5.

Table 5: LDT Comparison of DGP with NLO Crystals

Crystal	LDT(GW/cm^2)	References
DGP	3.36	Present worK
GPMG	2.35	(18)
Urea	1.5	(19)
TDGP	3.54	(20)
KDP	0.2	(18)
LADGP	2.6	(21)

Z-Scan Analysis

Z-scan approach was operated to delve the 3rd order NLO characteristics for the developed DGP single crystal. Utilizing a polarized Gaussian beam in TEM00 mode, a convex lens having a focal length of 300 millimeters was utilized to focus the beam, resulting in a beam waist of ω_0= 16.1 μm for DGP. The thickness of the crystal (L) was 1 millimeter for DGP, with the calculated Rayleigh length (ZR) determined to be 1.3 mm. The condition (L < ZR) prevailed across the negative (–Z) to positive (Z)

axis, parallel to the propagation direction of the laser beam. The translation of the sample holder was controlled by a computer, while the digital power meter recorded the corresponding transmitted intensity at each instance. The incident intensity within a closed aperture depended on the aperture radius (2 millimeter). Conversely, in an open aperture configuration, the detector swiftly gathered intensity to ascertain the nonlinear absorption coefficient (β). The refractive index for the DGP crystal and its absorption directly influenced the laser beam intensity (22-25). The sample induced a peak-to-valley variation in the closed aperture, indicating the presence of the self-defocusing effect (26), as illustrated in Figure 18. Conversely, in the open aperture setup, the DGP crystal exhibited the bottomost transmittance (valley) at the focal point (Z_0), demonstrating reverse saturable absorption, as depicted in Figure 19. This suggests that 'β' is positive. In the closed-aperture configuration, the third-order nonlinear refractive index 'n_2' was observed to be 3.85 × $10^{-12}m^2/W$ for DGP. Meanwhile, the nonlinear absorption coefficient in the open-aperture setup 'β' was determined to be 2.434 × 10^{-5}m/W for DGP. The magnitude of the 3rd order nonlinear susceptibility '$\chi^{(3)}$' was evaluated as 1.009 × 10^{-8}esu for DGP. The self-defocusing property of DGP crystals presents promising opportunities across diverse fields like nonlinear optics, laser technology, imaging, and photonics. Overall, this DGP crystal holds potential implications for telecommunications, imaging systems, and optical signal processing applications (27, 28).

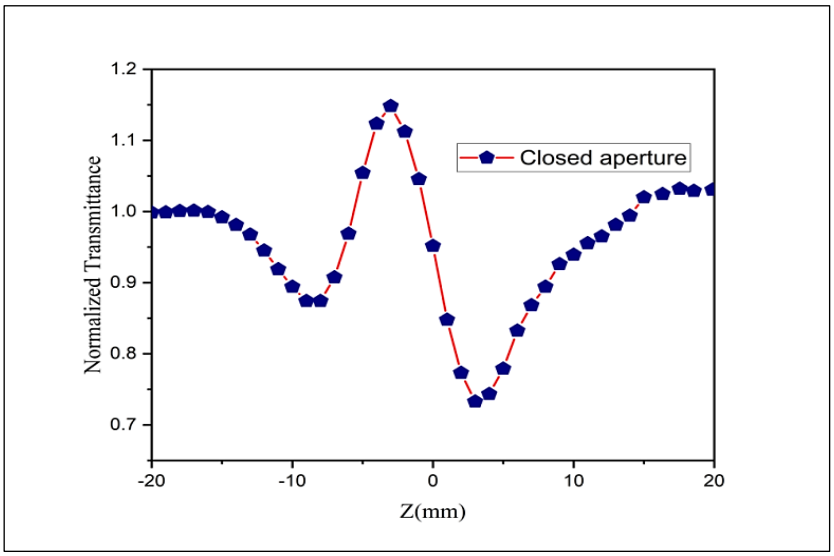

Figure 18: Closed Aperture Curve of DGP

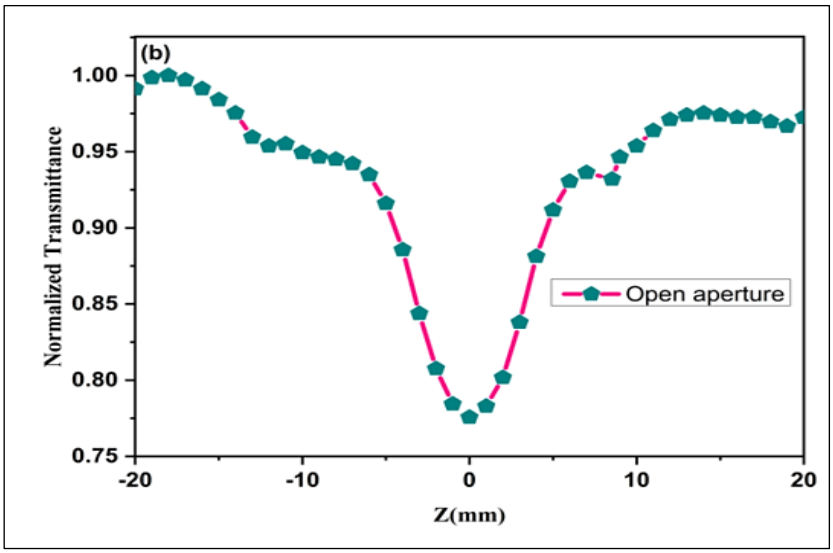

Figure 19: Open Aperture Curve of DGP

Conclusion

The optically good, superior-quality DGP single crystal was successfully grown using the slow evaporation solution technique, achieving dimensions of 10 mm × 9 mm × 3 mm. Single-crystal XRD confirmed the monoclinic structure, while powder XRD further validated the crystal's structural integrity. FTIR analysis verified the presence of functional groups and their corresponding vibrational modes. Mechanical stability was assessed using microhardness testing. UV–Visible–NIR spectroscopy revealed excellent optical transparency 98% with cut-off wavelengths at 235 nm and 350 nm, indicating strong potential for nonlinear optical (NLO) applications. Thermal analysis via TG-DTA demonstrated that the crystal is thermally stable up to 240 °C. The dielectric measurements indicated low dielectric loss at high frequencies, pointing to high optical quality with minimal internal defects. The third-order nonlinear optical susceptibility ($\chi^{(3)}$) was measured to be 1.009×10^{-8} esu, and the laser damage threshold (LDT) was calculated as 3.36 GW/cm^2.These results collectively highlights the DGP crystal's exceptional optical transparency, notable third-order nonlinear susceptibility, and robust thermal and mechanical stability—key attributes for nonlinear optical device applications. The distinctiveness of this work lies in the thorough characterization of the material, paired with impressive performance metrics such as $\chi^{(3)}$ and LDT values that surpass those reported for many similar materials. This establishes the DGP crystal as a strong contender for integration into advanced photonic technologies, including optical modulators, switches, and sensors. Additionally, its pronounced nonlinear optical response and low dielectric loss suggest a high level of crystalline quality, reinforcing its potential for high-efficiency optical applications.

Abbreviation

None.

Acknowledgement

None.

Author Contributions

All authors contributed equally to this work.

Conflict of Interest

The author has stated the absence of any conflict of interest.

Ethics Approval

Not applicable.

Funding

No funding received.

References

1. Ghazaryan VV, Fleck M, Petrosyan AM. Glycine glycinium picrate—Reinvestigation of the structure and vibrational spectra. Spectrochim Acta A Mol Biomol Spectrosc. 2011;78(1):128–32.
2. Shakir M, Muhammad S, AlFaify S, Irfan A, Khan MA, Al-Sehemi AG, Bdikin I. A comparative study of key properties of glycine glycinium picrate (GGP) and glycinium picrate (GP): A combined experimental and quantum chemical approach. J Saudi Chem Soc. 2018; 22(3):352–62.
3. Sivaraman S, Balakrishnan C, Prasad AA, Sokalingam RM, Meenakshisundaram SP, Markkandan R. Crystal growth, structure and characterization of diglycine zinc dipicrate: Centrosymmetric crystal exhibiting second harmonic generation efficiency. Mol Cryst Liq Cryst. 2017; 656(1):153–68.
4. Alen S, Sajan D, Umadevi T, Němec I, Baburaj MS, Jothy VB, Joy BS. Twisted intramolecular charge transfer and its contribution to the NLO activity of Diglycine Picrate: A vibrational spectroscopic study. Spectrochimica Acta Part A: Molecular and Biomolecular Spectroscopy. 2015 Jan 25; 135:720-31.
5. Dadsetani M, Omidi AR. Ab initio study on optical properties of glycine sodium nitrate: a novel semiorganic nonlinear optical crystal. RSC Advances. 2015; 5(110):90559-69.
6. Shakir M, Kushwaha SK, Maurya KK, Arora M, Bhagavannarayana G. Growth and characterization of glycine picrate—Remarkable second-harmonic generation in centrosymmetric crystal. J Cryst Growth. 2009; 311(15):3871–5.
7. Rajarajan K, Manimekalai B, Mohanadevi B, Madhurambal G. Synthesis and characterization studies on glycine picrate crystal doped with $CdCl_2$: A nonlinear optical material. Int J Pharm Chem Biol Sci. 2015;5(1):321–7.
8. Balasundari N, Selvarajan P, Ponmani SLM, Jencylin D. Studies on growth and characterization of urea-doped diglycine picrate (DGP) single crystals. Recent Res Sci Technol. 2011;3(12):64–6.
9. Devi TU, Lawrence N, Babu RR, Ramamurthi K. Growth and characterization of glycine picrate single crystal. Spectrochim Acta A Mol Biomol Spectrosc. 2008;71(2):340–3.
10. Chellam MKB, Gowri E, Thilagavathy SR. L-Lysine doped organic nonlinear optical crystal. Int J Eng Res Technol (IJERT). 2017; 5(15). https://www.ijert.org/l-lysine-doped-organic-nonlinear-optical-crystal
11. Rajarajan K, Babu K, Vijayalakshmi K, Arivudainambi T, Madhurambal G. Synthesis, growth and

characterization studies of thiourea picrate crystal. Int J Pharm Chem Biol Sci. 2017;7(2):90–5.
12. Thilagavathi R, Selvarajan P, Vasantha Kumari V. Influence of zinc chloride on the structural, optical, mechanical and NLO properties of diglycine picrate (DGP) single crystal. Int J Recent Sci Res. 2015;6(11):7436–9.
13. Athira KM, Naseema K. Growth, optical, thermal and mechanical studies of picric acid doped L-threonine single crystals. Int Res J Eng Technol. 2018;5:09.
14. Arulmani S, Senthil S. Growth and optical studies on L-leucine doped ADP single crystals for non-linear optical applications. Mater Today Proc. 2018; 5(2):8996–9003.
15. Raghavan R, Srinivasan S, Venkatakrishnan S, Panneerselvam K, Chandramouleeswaran S. Growth, structural, spectral, thermal, electrical and optical characterization of a novel optical material: Triethanolamine picrate single crystals for optical applications. Chin J Phys. 2020;67:27–36.
16. Chinnasami S, Chandran S, Paulraj R, Ramasamy P. Structural, vibrational, Hirshfeld surfaces and optical studies of nonlinear optical organic imidazolium L-tartrate single crystal. J Mol Struct. 2019;1179:506–13.
17. Kommandeur J. Photoconductivity in organic single crystals. Journal of Physics and Chemistry of Solids. 1961 Dec 1;22:339-49.
18. Law KY. Organic photoconductive materials: recent trends and developments. Chemical Reviews. 1993 Jan 1;93(1):449-86.
19. Yen WM, Raukas M, Basun SA, Van Schaik W, Happek U. Optical and photoconductive properties of cerium-doped crystalline solids. Journal of Luminescence. 1996 Dec 2;69(5-6):287-94.
20. Lasalle BSI, Karuppasamy P, Pandian MS, Ramasamy P. Investigation of structural, optical, and thermal properties of 2-amino-4,6-dimethylpyrimidine benzoic acid (2APB) single crystal for non-linear optical (NLO) applications. J Mater Sci Mater Electron. 2022;33(22):17780–92.
21. Thilagavathy SR, Rajesh P, Ramasamy P, Ambujam K. A study on Fourier transform infrared spectroscopy, thermal, mechanical, NLO and laser damage properties on unidirectional Glycinium Picrate Mono Glycine crystal. Spectrochimica Acta Part A: Molecular and Biomolecular Spectroscopy. 2013 Nov 1;115:747-52.
22. Suganthi R, Balasubramanian K. Multi-faceted characterization of thiourea-doped diglycine picrate (TDGP) single crystals for advanced nonlinear optical applications. Indian Journal of Physics. 2025 Jan 5;99(8):1-0.
23. Suganthi R, Balasubramanian K. Functional profiling of l-alanine diglycine picrate (LADGP) single crystal for nonlinear optical enhancement. Tuijin/Jishu Journal of Propulsion Technology.2024;45(3). https://www.propulsiontechjournal.com/index.php/journal/article/view/7702
24. Devi TU, Lawrence N, Babu RR, Ramamurthi K, Bhagavannarayana G. Structural, electrical and optical characterization studies on glycine picrate single crystal: a third order nonlinear optical material. J Miner Mater Charact Eng. 2009;8(10):755–63.
25. Priscilla J, Vijayaraghavan GV, Kumar KY. Influence of procion red dye doping on the structural, dielectric and optical properties of diglycine-phthalic acid single crystals for nonlinear optical applications. J Mater Sci Mater Electron. 2024;35(18):1265.
26. Ravi S, Sreedharan R, Raghi KR, Kumar TM, Naseema K. Experimental and theoretical studies on various linear and non-linear optical properties of 3-aminopyridinium 3,5-dinitrobenzoate for photonic applications. Braz J Phys. 2021;51:22–39.
27. Kubendiran T, Ravi Kumar SM, Allen Moses SE, Nasareena Banu A, Shanthi C, Sivaraj S. Second and third order nonlinear optical, mechanical, surface characteristics of bis(thiourea) manganese chloride (BTMC) grown by slow cooling technique used for frequency conversion applications. J Mater Sci Mater Electron. 2019;30:17559–71.
28. Babu B, Chandrasekaran J, Thirumurugan R, Jayaramakrishnan V, Anitha K. Experimental and theoretical investigation on 2-amino 5-bromopyridinium L-tartrate—A new organic charge-transfer crystal for optoelectronics device applications. J Mater Sci Mater Electron. 2017;28:1124–35.